

Assessment of the Accuracy of Dental Enamel Thickness Measurements Using Microfocal X-Ray Computed Tomography

ANTHONY J. OLEJNICZAK^{1*} AND FREDERICK E. GRINE^{2,3}

¹Interdepartmental Doctoral Program in Anthropological Sciences, Stony Brook University, Stony Brook, New York

²Department of Anthropology, Stony Brook University, Stony Brook, New York

³Department of Anatomical Sciences, Stony Brook University, Stony Brook, New York

ABSTRACT

Tooth enamel thickness has long been an important character in studies of primate and especially hominin phylogeny, taxonomy, and adaptation. Current methods for accurately assessing enamel thickness involve the physical sectioning of teeth, because measurements of enamel thickness using some radiographic techniques are unreliable. However, because destructive methods limit sample sizes and access to important fossil specimens, it is desirable that they be replaced with nondestructive techniques. Although microfocal X-ray computed tomography (mCT) has been used recently in studies of enamel thickness, the accuracy of this technique has yet to be established. The present research compares physical sections to computer-generated mCT sections of teeth from a variety of primate and nonprimate, recent and fossil taxa to examine whether enamel thickness, tooth size, and diagenetic remineralization (fossilization) impact the ability of mCT to measure enamel thickness accurately. Results indicate that recent teeth of varying size and thickness are clearly and accurately depicted in mCT scans, with measurements from nearly identical planes in physical and mCT sections differing by 3–5%. A fossil papionin molar (ca. 2 Myr) was also accurately measured using mCT scans, although thinner enamel in much older therapsid (ca. 263–241 Myr) teeth could not be distinguished from dentine. mCT is thus an accurate technique for measuring enamel thickness in recent taxa, although heavily mineralized teeth pose an obstacle to the ability of mCT to distinguish dental tissues. Moreover, absolutely thin enamel (less than ~ 0.10 mm) is difficult to resolve adequately in raw mCT images based on pixel values alone. Therefore, caution must be exercised in the application of mCT to the study of fossilized teeth. © 2006 Wiley-Liss, Inc.

Key words: mCT; microfocal X-ray computed tomography; enamel thickness; measurement accuracy; diagenesis; dental enamel; dentine

Tooth enamel thickness has long been considered to be of importance in the interpretation of human evolution because of its purported taxonomic and phylogenetic value (Miller, 1918; Simons and Pilbeam, 1972; Kay, 1981; Gantt, 1983; Martin, 1985; Beynon and Wood, 1986; Grine and Martin, 1988; Zilberman et al., 1990; Beynon et al., 1991; Macho and Thackeray, 1992; Zilberman and Smith, 1992a, 1992b, 1994; Zilberman et al., 1992; Macho and Berner, 1993; Molnar et al., 1993; Smith and Zilberman, 1994; White et al., 1994; Strait et al., 1997; Shellis et al., 1998; Haile-Selassie, 2001; Senut et al., 2001; Strait and Grine, 2001, 2004; Brunet et al., 2002; Wolpoff et al., 2002; Martin et al., 2003; Haile-Selassie et al., 2004). Enamel thickness is also thought to be of significance for the

interpretation of occlusal loading regimens (Schillingburg and Grace, 1973; Molnar and Gantt, 1977; Kay, 1981; Grine and Martin, 1988; Khera et al., 1990; Macho and

*Correspondence to: Anthony J. Olejniczak, Interdepartmental Doctoral Program in Anthropological Sciences, Stony Brook University, Stony Brook, NY 11794. Fax: 631-632-9165. E-mail: aolejnic@ic.sunysb.edu

Received 25 April 2005; Accepted 17 November 2005
DOI 10.1002/ar.a.20307
Published online 6 February 2006 in Wiley InterScience (www.interscience.wiley.com).

Berner, 1993; Dumont, 1995; Spears and Macho, 1998; Macho and Spears, 1999; Schwartz, 2000a, 2000b; Martin et al., 2003).

Physical cross-sections of molar teeth have been used to measure enamel thickness by a number of workers (e.g., Molnar and Gantt, 1977; Martin, 1985; Beynon and Wood, 1986; Grine and Martin, 1988; Macho and Berner, 1993; Dumont, 1995; Schwartz, 2000b; Grine, 2002, 2004, 2005; Grine et al., 2005). Physical sections provide an accurate portrayal of enamel thickness in a particular plane of section, but problems with specimen orientation (i.e., section obliquity) may render some of these data less than ideal. Moreover, because mechanical sectioning is destructive, even when the cut is as narrow as 70 μm (Grine and Martin, 1988), it is difficult to obtain adequate samples for statistical comparison, especially when the taxa under consideration are rare, endangered, or extinct.

Alternative techniques have been developed and employed in response to the problem of accurately reconstructing enamel cap volumes from physical sections, although some of these entail the destruction of the entire enamel cap (Kono-Takeuchi et al., 1997; Kono et al., 2002). Noninvasive methods such as ultrasonic imaging or acoustic microscopy (Baum et al., 1963; Lees, 1968, 1971; Lees and Barber, 1968; Peck et al., 1989; Yang, 1991, 1996; Mezava et al., 1999; Maev et al., 2000, 2002) and radiography have been employed to quantify tooth enamel thickness. Although acoustic microscopy has been used in several clinical studies of enamel and dentine, the accuracy of the quantitative data obtained has yet to be established. Various radiographic techniques have been employed extensively in the measurement of tooth enamel thickness to address clinical as well as evolutionary questions, including flat-plane radiography, computed tomography, and, most recently, microfocal X-ray computed tomography (mCT).

Lateral flat-plane radiographs have been used to measure enamel thickness in living humans. Standard biting radiographs of dental patients have been used to study the effect of sex-linked genes on tooth size (Alvesalo and Tammisalo, 1981; Alvesalo, 1985; Alvesalo et al., 1985, 1987), and they also have been used to assess the effects of sex and ethnic background on tooth crown components (Stroud et al., 1994, 1998; Zilberman and Smith, 1994; Harris and Hicks, 1998; Harris et al., 1999). Lateral flat-plane radiographs also have been used to measure enamel thickness in fossil hominin and hominoid specimens (Sperber, 1985, 1986; Nagatoshi, 1990; Zilberman et al., 1990; Zilberman and Smith, 1992b, 1992a; Molnar et al., 1993; Faerman et al., 1994; Smith and Zilberman, 1994). These studies utilized the parallel-film technique, in which the film is oriented parallel to the major axis of the tooth, and the X-ray beam is directed perpendicular to an imaginary plane that bisects the vertical and mesiodistal axes of the tooth and the plane of the radiographic plate (Gron, 1960). Some studies have recorded linear measurements from lateral radiographs, while others have measured the projected area of the enamel cap. It has been shown, however, that measurements of enamel thickness from standard lateral radiographs are unlikely to reflect accurately the true thickness as defined by physical sections through the crown (Grine et al., 2001). Thus, while this type of X-ray may provide a qualitative impression of whether a tooth has relatively thin enamel (e.g., human deciduous molars) or relatively thick enamel (e.g.,

human permanent molars), measurements derived from standard lateral radiographic images are unlikely to reflect that thickness accurately.

Computed tomography (CT) has also been utilized to quantify enamel thickness in recent and fossil hominin teeth (e.g., Zonneveld and Wind, 1985; Conroy, 1991; Conroy and Vanier, 1991; Macho and Thackeray, 1992; Conroy et al., 1995; Schwartz et al., 1998). With the exception of the study by Schwartz et al. (1998), however, these analyses have employed standard CT scans, a technique that has been demonstrated to be grossly inaccurate in the measurement of enamel thickness (Grine, 1991). Standard CT images generally exaggerate enamel thickness compared to values obtained from mechanical sections (Grine, 1991). There are several reasons for this, including beam hardening artifacts, partial volume effect, and the improbability of obtaining a CT slice that traverses the tips of both dentine horns (Grine, 1991). Moreover, Spoor et al. (1993) have shown that accurate linear measurements of enamel can be obtained with CT scans only if the half maximum height (HMH) values are calculated between adjacent CT number levels at both the air-enamel and enamel-dentine boundaries. Failure to image at the proper HMH CT values can result in measurement errors in excess of 1.0 mm (Spoor et al., 1993). Even when the correct HMH CT adjustment is used, thin enamel cannot be measured accurately (its thickness will be exaggerated) due to limited spatial resolution of the scanner (Spoor et al., 1993). These factors render suspect the results of enamel thickness measurements reported in a number of studies that did not take them into account (e.g., Zonneveld and Wind, 1985; Conroy, 1991; Conroy and Vanier, 1991; Macho and Thackeray, 1992; Conroy et al., 1995).

Technical advances in computer-assisted radiographic techniques have resulted in the application of microfocal X-ray computed tomography as a nondestructive technique for the measurement of enamel thickness (Chaimanee et al., 2003; Gantt et al., 2003; Kono, 2004; Olejniczak and Grine, 2005). The intricate structure of cancellous bone has been extensively studied using mCT (Kuhn et al., 1990; Bonse et al., 1994; Müller et al., 1996a,b; Rügsegger et al., 1996; Müller and Rügsegger, 1997; Kappelmann, 1998; Kinney et al., 1998; Fajardo and Müller, 2001; MacLachy and Müller, 2002; Müller, 2002, 2003), and this technology has even been applied successfully to the visualization of the brain endocast and vestibular apparatus of Mesozoic pterosaurs (Witmer et al., 2003).

A number of studies have examined the repeatability of measurements (and inter- and intraindividual errors in locating landmarks) from mCT images of trabecular bone (e.g., Durand and Rügsegger, 1991; Balto et al., 2000), tooth root canals (Peters et al., 2000), and tooth enamel (Avishai et al., 2004). To date, however, the only studies that have attempted to assess the accuracy of measurements derived from high-resolution X-ray computed tomography have been conducted with reference to trabecular bone configuration (Kuhn et al., 1990; Müller et al., 1996a,b, 1998; Hildebrand et al., 1999; Fajardo et al., 2002), periapical and periradicular alveolar bone destruction (Balto et al., 2000; von Stechow et al., 2003), the diameters of tooth root canals (Rhodes et al., 1999), and cortical bone porosity (Cooper et al., 2004). We are unaware of any study that has addressed the issue of measurement accuracy in the mCT assessment of dental hard tissues.

TABLE 1. Study sample and average published measurements

Taxon	Age	Tooth	BCD* (mm)	Maximum Lateral Linear Enamel Thickness (mm)
<i>Alligator mississippiensis</i>	Recent	Caniniform	6.60	0.14
<i>Ateles paniscus</i>	Recent	LM ₁	4.20	0.40
<i>Cebus apella</i>	Recent	LM ₂	4.50	0.90
<i>Chiropotes satanus</i>	Recent	LM ₁	2.70	0.30
<i>Crocodylus palustris</i>	Recent	Caniniform Maxillary	6.70	0.24
<i>Diademodon tetragonus</i>	c. 241 Myr	Molariform	8.90	0.05
<i>Homo sapiens</i>	Recent	LM ³	10.90	0.60
<i>Homo sapiens</i>	Recent	RM ₃	8.90	2.20
<i>Homo sapiens</i>	Recent	Ldm ₁	5.90	0.70
<i>Moschops capensis</i>	c. 263 Myr	Incisor	8.50	0.36
<i>Papio robinsoni</i>	c. 2.0 Myr	LM ₂	10.00	0.90
<i>Papio ursinus</i>	Recent	LM ²	12.70	1.70

* Bi-cervical diameter, see definition in figure 2.

Kuhn et al. (1990), Müller et al. (1996a,b, 1998), Hildebrand et al. (1999), and Fajardo et al. (2002) observed negligible differences between measurements derived from mCT images and those obtained using traditional histomorphometric or stereological techniques applied to histological thin sections. Percentage differences between the mCT and histological values reported by these studies ranged between lows of 0.88–1.17 (Müller et al., 1996a,b) and highs of 2.5–6.1 (Müller et al., 1996a,b), depending upon the type of physical section examined. Balto et al. (2000) and von Stechow et al. (2003) also reported negligible differences between measurements obtained from mCT and histological sections of periapical and periradicular bone. Rhodes et al. (1999) similarly reported very high correlations between the values recorded for the diameters of tooth root canals from mCT images and physical sections. Cooper et al. (2004) compared measurements obtained by mCT to those recorded from microradiographs of cortical bone, and while the two methods produced similarities, relatively poor results were obtained for measurements of pore density. Unfortunately, it is not possible to ascertain the source of this discrepancy or its deviation from values derived from physical sections because histological preparations were not measured directly. Fajardo et al. (2002) concluded that mCT can accurately reconstruct the complex architecture of trabecular bone, although slight alterations in threshold values greatly affected the morphometric data.

The only mCT studies that have been directed explicitly at the resolution of dental hard tissues (e.g., Avashai et al., 2004; McErlain et al., 2004) have not involved comparisons of measurements derived from mCT and physical sections. McErlain et al. (2004) examined a single tooth from a 420-year-old Late Iron Age site in Cambodia and simply commented that they were clearly able to differentiate visually the hard tissue components, which were displayed with “exceptional clarity.” The study by Avishai et al. (2004) examined individual error rates in locating landmarks (and resultant measurements) in a series of tooth germs derived from archeological contexts.

Thus, although mCT is a potentially powerful tool by which to obtain information on enamel thickness in a nondestructive manner, its efficacy for this purpose has yet to be demonstrated. It is necessary to establish the validity of enamel thickness measurements obtained us-

ing mCT before these data are employed to answer questions of clinical or evolutionary interest. The purpose of the present study was to establish the accuracy of high-resolution mCT for the measurement of enamel thickness in teeth of differing size, enamel thickness, and degree of mineralization. Toward this end, we compared measurements obtained from mCT scans that had not undergone any image artifact corrections (as this may impact measurements) to those obtained from physical sections of the same specimens. In the first instance, we measured mCT and histological sections using standard techniques (i.e., measuring printed images using a digitizing tablet) in order to make our results comparable to those of previously published studies. As mCT studies become more common, direct measurement by means of computer software will also become commonplace. We therefore also compared our measurements obtained by digitization to those taken directly on the three-dimensional models in order to assess the comparability of these protocols.

MATERIALS AND METHODS

Study Sample Composition

Twelve isolated teeth that varied in size, absolute enamel thickness, and degree of mineralization were chosen for study (Table 1). One of the modern human molars (Fig. 1) was embedded in a cylinder of methyl methacrylate. Although the absolute sizes of the teeth differed somewhat, all were chosen for their ability to be accommodated within the specimen tubes of the mCT system that was used (μ CT 40; Scanco Medical, Switzerland). These tubes range from 13 to 35 mm in diameter. Beyond this, the extant primate and sauropsid specimens were selected on the basis of published values (Dauphin, 1987; Sato et al., 1988; Shellis et al., 1998; Martin et al., 2003; Grine, 2005; Grine et al., 2005) and personal observations of enamel thickness, such that a range of thin- to thick-enamed teeth was represented. The three fossil teeth were chosen on the basis of absolute enamel thickness and geological age, with the latter expected to exhibit some degree of correlation with degree of diagenetic remineralization.

The fossil baboon specimen derives from the site of Bolt's Farm, South Africa, and dates to approximately 2.0 Myr ago (Delson, 1984, 1988). The specimen (University of California Museum of Paleontology, UCMP 56773) is most

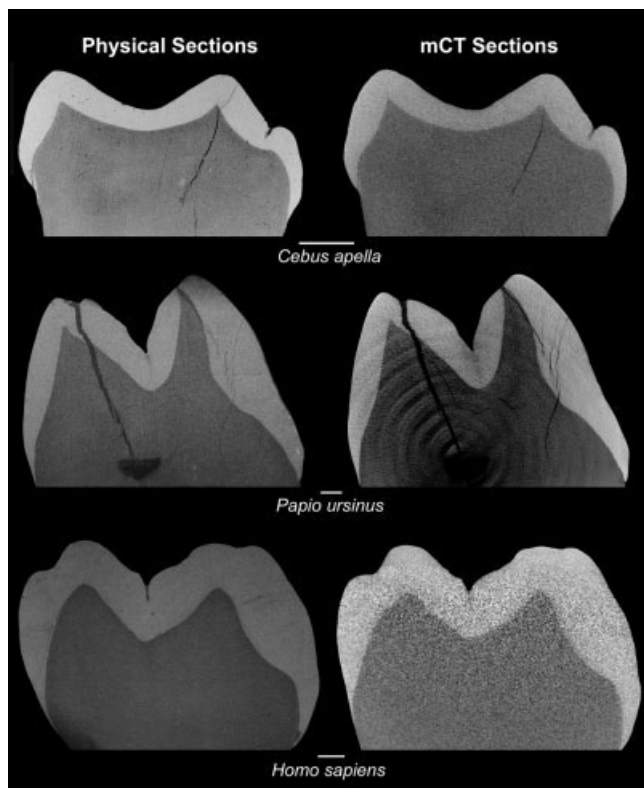


Fig. 1. Scanning electron micrographs (left) and mCT images of the same cross-section through three of the primate molars examined. Scale bar = 1 mm.

likely attributable to *Papio robinsoni* (E. Delson, personal communication). The two therapsid teeth are from the Permo-Triassic sediments of the Karoo Basin of South Africa. The younger of the two specimens (National Museum, Bloemfontein, specimen QR 1222) is a molariform tooth of the cynodont *Diademodon tetragonus*, the enamel of which is extremely thin (Grine et al., 1979). This fossil dates to the Early-Middle Triassic boundary (Lucas, 1995), or the Early Anisian, between some 237 and 245 Myr (Hancox and Rubidge, 2001; De Kock et al., 2003; Rubidge, 2005). The older of the two therapsid specimens (South African Museum, Cape Town, specimen K 203) is an isolated tapinocephalid incisor. It derives from the Abrahamskraal Formation of the Beaufort Group and dates to the Middle Permian (Smith and Keyser, 1995), or Capitanian, between about 260 and 266 Myr (Hancox and Rubidge, 2001; De Kock et al., 2003; Rubidge, 2005). The incisor is compatible with assignment to either *Struthiocephalus whaitsi* or *Moschops capensis*; because the latter is more common in these strata (Smith and Keyser, 1995), we assign the tooth to it.

Physical Cross-Section and mCT Image Acquisition

In order to generate a three-dimensional model of each tooth, every specimen was scanned in its entirety using a fan-beam-type desktop mCT system (μ CT 40; Scanco Medical). The diameter of the specimen tubes used, as well as the voxel dimensions and number of slices produced, are

given in Table 2. All scans were output with $2,048 \times 2,048$ pixels per slice and 8 bits per pixel; the resultant voxels were isometric (having identical length, width, and depth). Each scan used the same settings for voltage (50 kV) and amperage (160 μ A), and the acquisition time for each slice was 4–7 sec, with a reconstruction time of approximately 24 sec per slice at an angular increment of 0.36° . After the mCT scanning of each tooth was complete, the specimens were prepared for physical sectioning following established methods (Grine, 2005). The tips of the two mesial cusps (protocone and paracone, or metaconid and protoconid) of the primate molars were marked with a spot of permanent ink. An equivalent procedure was employed for the sauropsid and therapsid teeth, taking into account the fact that because they differ morphologically from the primate molars, a homologous plane is not available. In these instances, a series of anatomical landmarks and pseudolandmarks (e.g., cusp tips, cervical margins) was identified in order to define the location of the plane of section. The crown was then embedded in epoxy and sectioned with a 0.15 mm diamond-wafering blade (Buehler Isomet). The blade was positioned immediately distal to the ink marks to ensure that the mesial crown block included both dentine horns. This block face was ground with 400-grade paper and polished with a sequence of diamond pastes to 0.25 μ m (Buehler Microcloth) to obtain a topography-free buccolingual (BL) section that traversed the tips of both dentine horns (in the case of the primate molars). The polished surface was lightly etched with 0.5% H_3PO_4 for 15 sec to remove any smeared enamel, ultrasonicated in distilled H_2O , mounted on a stub, and coated with silver for examination by scanning electron microscopy (AMRAY 1810). These specimens were examined at 25 kV in either secondary or, more commonly, back-scattered electron mode. Micrographs were recorded using Polaroid type 55 P/N film at magnifications between $7.5\times$ and $11.0\times$, depending on the size of the specimen; working distance was held under 27 mm to ensure accurate magnification. Enlargements of the micrographs were used for measurement.

In order to compare measurements recorded from the physical sections to those obtained by mCT, stacked image sequences of each tooth derived from mCT scanning were imported into the VoxBlast software program (Vaytek) to create three-dimensional reconstructions of the crown. The size of the mCT image file at the slice thicknesses used here (3.0–10.0 GB for each image stack in this study) imposes certain hardware limitations, so image stacks were stored at a resolution of 512×512 pixels [(the same pixel dimensions used by Kono (2004)] rather than the $2,048 \times 2,048$ pixels generated by the mCT unit. We noted no visual loss of image quality after the adjustment. Because the slice thickness of the scans was preserved, the pixel size was effectively four times the slice thickness. All VoxBlast procedures described here were performed on a computer equipped with a 2.8 GHz Hyper-Threading Pentium IV processor (Intel) and 2.0 GB of random access memory.

VoxBlast software allows user-defined planes of section to be created, and these can pass through the three-dimensional reconstructions at any orientation. Using two enamel cusp tips as landmarks (in the case of the primate molars), a buccolingual section was made through each tooth model, attempting to capture the same plane as was located in the physical sections. An iterative (slice-by-

TABLE 2. mCT scanning protocol

Taxon	Tooth	Tube Diameter (mm)	Voxel Dimension (mm)	Post-Processing Pixel Resolution (mm)	Scan Length (mm)
<i>Ateles paniscus</i>	LM ₁	12.3	0.0060	0.0240	6.6
<i>Cebus apella</i>	LM ₂	12.3	0.0060	0.0240	4.0
<i>Chiropotes satanus</i>	LM ₁	12.3	0.0060	0.0240	4.6
<i>Homo sapiens</i>	LM ³	16.4	0.0080	0.0320	10.5
<i>Homo sapiens</i>	Ldm ₁	16.4	0.0080	0.0320	6.8
<i>Homo sapiens</i>	RM ₂	20.5	0.0100	0.0400	15.9
<i>Papio ursinus</i>	LM ²	20.5	0.0100	0.0400	14.5
<i>Crocodylus palustris</i>	Caniniform	20.5	0.0100	0.0400	3.4
<i>Alligator mississippiensis</i>	Caniniform	20.5	0.0100	0.0400	3.4
<i>Diademodon tetragonus</i>	Molariform	16.4	0.0080	0.0320	16.2
<i>Moschops capensis</i>	Incisor	35.0	0.0175	0.0700	1.1
<i>Papio robinsoni</i>	LM ₂	20.5	0.0100	0.0400	15.7

slice) technique was employed to refine the location of this plane of section based on visual comparison of the SEM micrographs to the mCT model. Anatomical landmarks unique to a particular plane (e.g., cracks in the enamel or dentine, distinct pulp chamber morphology, distinct dentine topography) were identified in order to match the mCT section to the physical section. After locating the desired plane of section in the mCT model, the image of this plane was exported and printed at its resolution based on our postprocessing technique (512×512 pixels). Two images representing the same plane of section were thus available for comparison for each specimen: one generated by physical sectioning and one generated by mCT (Fig. 1).

As mCT analysis of teeth becomes commonplace, the measurement of dental tissues using software alone (rather than digitizing a printed image) is likely also to become widespread. Therefore, we compared measurements that were recorded using both techniques to see whether they differ. Measuring the mCT sections and the SEM images of the histological sections using a digitizing tablet served to control potential sources of measurement error by ensuring that identical techniques were used to measure both sets of images. Digitization also made the method of analysis used here comparable to that of previous studies. We then compared digitized measurements with on-screen measurements in order to establish whether the data derived from these two techniques are equivalent. Certain measurements that are based on anatomical landmarks (e.g., the thickness of enamel between the dentin horn tip and the enamel cusp tip) were recorded on the mCT images for three of the specimens using Vox-Blast software. These values were compared to measurements obtained by digitizing the printed images.

Measurements Recorded

Measurements describing the thickness of enamel relative to other dental dimensions were recorded for each primate molar (Fig. 2). These include the area of coronal dentine and pulp (b), the area of the enamel cap (c), and the bicervical diameter (BCD). Eleven measurements describing the linear thickness of enamel at various locations across the molar crown were also recorded for each primate tooth. Because different absolute enamel thicknesses are accompanied by differential rates of error using standard CT methods (Grine, 1991; Spoor et al., 1993), the

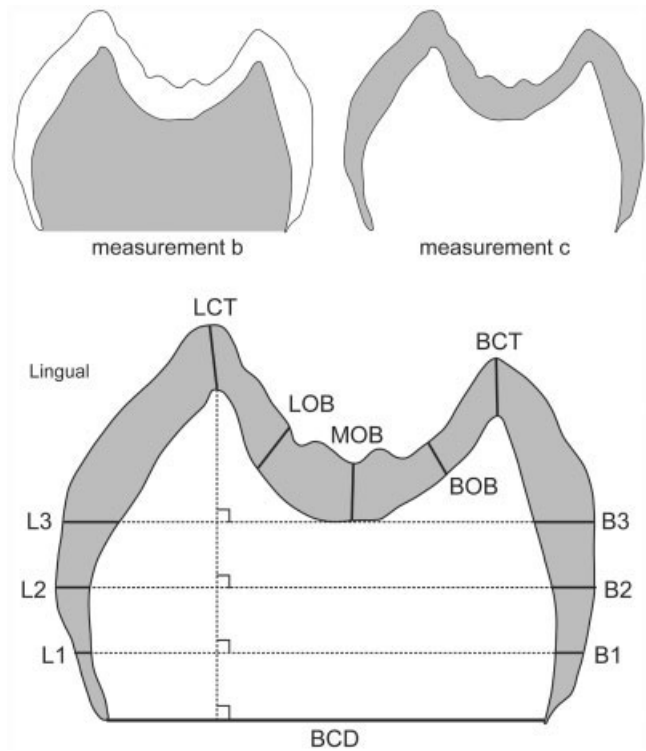


Fig. 2. Schematic diagram of the enamel thickness measurements recorded in the primate teeth examined. Measurement b is the area of dentine (including the area of the pulp chamber, if present in the section) contained within the enamel cap (in mm^2). Measurement c is the area of enamel in cross-section (in mm^2). BCD is the bicervical diameter, the distance between the two enamel cervices (in mm). LCT and BCT are the linear thicknesses of enamel between the dentine horn apex and the enamel cusp tip in the lingual and buccal cusps, respectively (in mm). LOB, MOB, and BOB are the maximum radial enamel thickness in the lingual cusp occlusal basin, the mid-occlusal basin, and the buccal cusp occlusal basin, respectively (in mm). L1–L3 and B1–B3 are defined as the thickness of enamel at three evenly spaced intervals between the bicervical diameter and the lowest point of the enamel-dentine junction in the mid-occlusal basin, parallel to the bicervical diameter.

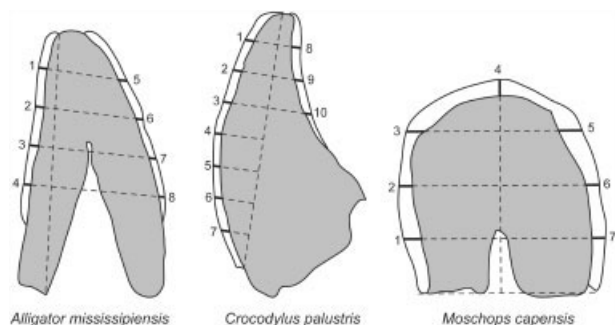


Fig. 3. Schematic diagram of the measurements recorded on the sauropsid and therapsid teeth examined in this study (not drawn to scale). Each measurement point was determined by first identifying two landmarks on each tooth (e.g., the labial enamel cervix and the cusp tip in the *Crocodylus* tooth), which form a reference line, and then drawing perpendicular lines through the crown at equally spaced intervals along this line, measuring the thickness of enamel where each perpendicular courses through the enamel cap.

linear measures were devised to examine whether areas of thick and thin enamel in an individual tooth yield comparable rates of measurement error using mCT. In the case of the fossil cercopithecoïd molar, the plane of section on which we took measurements coursed through the distal cusps due to postmortem breakage of the mesial half of the tooth. The morphology of extant sauropsid and fossil therapsid teeth is not comparable to that of primates, so a unique set of linear enamel thickness measurements was defined for comparing the two planes of section for each of these teeth (Fig. 3).

All measurements were recorded on enlargements of physical section micrographs and the printed mCT sections using SigmaScan software (Systat Software) interfaced with a SummaSketch III digitizing tablet (Cal-Comp). Values were recorded to the nearest 0.1 mm (or 0.1 mm²). Measurements derived from scanning electron microscopy were calibrated using the measurement scale printed on the micrographs. Measurements derived from mCT models were calibrated by the bicervical diameter of the image. This was determined using VoxBlast, as the number of pixels spanning the bicervical diameter related to the pixel size in microns. In order to minimize intraobserver error, each measurement was recorded three times, and the mean of these three trials was recorded as the value. In order to eliminate the potentially confounding effect of image manipulation on the resulting measurements, we did not attempt to enhance any image by eliminating scan artifacts (e.g., the ring artifacts evident in the *Papio ursinus* scan in Fig. 1), or by sharpening borders through the use of automated image filtering techniques.

Evaluation of Fossilized/Mineralized Enamel

The relative difference in density of enamel and dentine impacts directly the ability of mCT (or any X-ray-based radiographic technique) to distinguish these tissues. The relative densities of dentine and enamel were measured with OsiriX software (v1.6) (Rosset et al., 2004) on an Apple Macintosh computer. A single mCT cross-section of each fossil tooth, the two sauropsid teeth, and an extant primate molar were analyzed using OsiriX by tracing a region of interest (ROI) line over the cross-section, ensur-

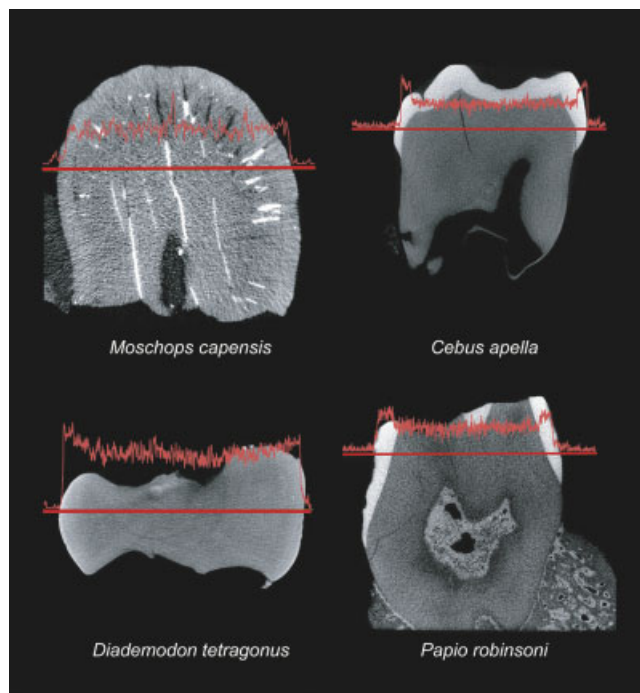


Fig. 4. Plots of the pixel values along region of interest lines in representative teeth. The height of the red line corresponds to the value of the pixels along the base line (higher values indicate a color value that is closer to white, lower values indicate closer to black). Note that in the extant *Cebus apella* molar and the fossil *Papio robinsoni* molar, the enamel clearly has higher pixel values than the dentine. Neither of the therapsid teeth shows a clear difference between enamel and dentine, although a postmortem fissure propagated between the enamel and dentine of the *Moschops capensis* incisor allows the two tissues to be separated for measurement.

ing that the line traversed both the enamel and the dentine. The value of each pixel crossed by the line (0 for black pixels, 255 for white pixels, and between 0 and 255 for shades of gray) was exported into a spreadsheet and plotted against its location on the line. The resulting charts were superimposed onto the mCT images of the teeth (Fig. 4). Substantial differences in the pixel values for enamel and dentine imply that they are heterogeneous in their density and therefore discernable for measurement, whereas like-valued pixels for enamel and dentine are not distinguishable by the mCT scanner.

RESULTS

Among the recent primate and sauropsid teeth, the enamel-dentine junction and outer enamel surface (hence the thickness of enamel) were clearly visible (e.g., Figs. 1 and 4). Scans of the modern human tooth that had been embedded in methyl methacrylate had more image noise than the other specimens, although measurements did not seem to be affected. Comparisons between the measurements derived from mCT images and physical sections are presented in Tables 3 and 4. The percentage difference between the mCT-derived and the physical section-derived measurements, expressed as an average of the 130 total measurements recorded, was 3.52% across the extant sample. As can be seen from the tables, there was no

TABLE 3. Values of measurements and percent differences between physical and mCT sections in recent primate teeth

Measurement	<i>Ateles paniscus</i>		<i>Cebus apella</i>		<i>Chiropotes satanus</i>		<i>Homo sapiens M³</i>		<i>Homo sapiens M₃</i>		<i>Homo sapiens dm₂</i>		<i>Papio ursinus</i>			
	mCT	Physical	% Diff.	mCT	Physical	% Diff.	mCT	Physical	% Diff.	mCT	Physical	% Diff.	mCT	Physical	% Diff.	
b	12.27	12.20	0.57%	7.49	7.27	3.03%	5.68	5.50	3.27%	39.14	40.99	4.51%	27.59	28.45	3.02%	
c	2.72	2.69	1.12%	3.67	3.57	2.80%	1.42	1.32	7.58%	30.29	30.57	0.92%	7.65	7.83	2.30%	
BCD	4.25	4.19	1.43%	4.64	4.55	1.98%	2.88	2.74	5.11%	9.38	8.87	5.75%	5.65	5.90	4.24%	
LCT	0.22	0.21	4.76%	0.57	0.57	0.00%	0.16	0.16	0.00%	1.94	1.60	5.00%	0.22	0.21	4.76%	
LOB	0.24	0.24	0.00%	0.48	0.48	0.00%	0.15	0.14	7.14%	1.45	1.62	4.94%	0.44	0.42	4.76%	
MOB	0.35	0.33	6.06%	0.40	0.39	2.56%	0.21	0.19	10.53%	0.90	0.89	1.12%	0.36	0.35	2.86%	
BOB	0.29	0.28	3.57%	0.45	0.46	2.17%	0.09	0.09	0.00%	2.29	2.34	2.14%	0.39	0.39	0.00%	
BCT	n/a	n/a	n/a	0.56	0.55	1.82%	n/a	n/a	n/a	1.98	1.74	6.75%	0.41	0.40	2.50%	
L1	0.23	0.24	4.17%	0.18	0.17	5.88%	0.16	0.17	5.88%	n/a	0.27	6.90%	0.37	0.39	5.13%	
L2	0.31	0.30	3.33%	0.31	0.29	6.90%	0.18	0.18	0.00%	n/a	0.78	2.63%	0.52	0.56	7.14%	
L3	0.39	0.40	2.50%	0.52	0.50	4.00%	0.19	0.18	5.56%	0.44	1.23	0.82%	0.58	0.60	3.33%	
B1	n/a	n/a	n/a	0.18	0.19	5.26%	0.14	0.13	7.69%	n/a	0.46	2.17%	0.33	0.35	5.71%	
B2	0.23	0.22	4.55%	0.27	0.27	0.00%	0.20	0.19	5.26%	0.30	0.86	2.27%	0.57	0.56	1.79%	
B3	0.37	0.38	2.63%	0.93	0.89	4.49%	0.30	0.31	3.23%	2.04	2.23	8.52%	0.71	0.74	4.05%	
Average (Absolute Value)			2.89%			2.92%			4.71%			4.66%			3.69%	2.96%

tendency for smaller teeth (e.g., *Ateles paniscus* mean difference = 2.89%) to have more or less percentage difference between measurements than larger teeth (e.g., *Papio ursinus* mean difference = 2.96%). There was no tendency for thick-enamelled teeth (e.g., *Homo sapiens M³* mean difference = 4.66%) to have less measurement difference than thin-enamelled teeth (e.g., *Chiropotes satanus M₁* mean difference = 4.71%). Moreover, there was no consistent pattern of mCT measurements being either smaller or larger than those taken on physical sections.

Across the different measurements taken, there is no obvious trend toward thinner regions of enamel being more prone to differences in measurements than thicker areas of the same tooth among the recent primate specimens. Measurements L1, L2, and L3, which represent the linear thickness of lingual enamel from nearer to the cervix to nearer to the cusp, respectively, showed an overall decrease in percent difference, although the same was not true for buccal measurements. Moreover, the increase from L1 to L3 was not substantial, although samples are not large enough to facilitate statistical comparisons. Area measurements (measurements b and c) tend to have lower percent differences than linear enamel thickness measurements.

Recording distance measurements using known landmarks on the computer screen (i.e., directly on mCT volume models in VoxBlast) did not result in substantially different measurements from those obtained by digitizing printed images (Table 5). There is, on average, from 2.60% to 3.50% difference between measurements taken on-screen and those using a digitizing tablet. These differences accord with those between the mCT prints and physical sections, as noted above.

There is a substantial difference between the ability of computer software (e.g., OsiriX, VoxBlast) and the human eye to distinguish enamel from dentine if scans are not first treated with some segmentation routine. Figure 5 depicts the physical and mCT-derived sections of the Alligator tooth, in which one can readily differentiate enamel from the underlying dentine. Also depicted is an ROI line through the same tooth, demonstrating that although the very thin enamel (as thin as 40 μm; Table 4) on the lingual surface is visible to the eye, the software is unable to distinguish the value of the enamel pixels from those of the dentine. This problem becomes important if computer software alone is used to record measurements, such as the volume of the enamel cap. A computer-rendering of the Alligator tooth is depicted in Figure 5; this demonstrates that although enamel is visible to the human eye on the lingual surface of the tooth, software alone (without any tissue segmentation) is incapable of differentiating it from the underlying dentine.

With regard to the mCT images of the fossil teeth (Table 6), while the extant primate molars evince a strong contrast between dentine and enamel, there is less contrast along the ROI line in the 2.0-Myr-old *Papio robinsoni* molar (Fig. 4). Nevertheless, the enamel cap was clearly visible on this fossil baboon crown in comparison to the substantially older Karoo fossils. Enamel could barely be distinguished from the underlying dentine in the *Moschops capensis* incisor, and this distinction was accentuated somewhat by their partial physical separation along a postmortem fissure (Fig. 4). The *Diademodon tetragonus* tooth crown was a homogeneous gray across the entire

TABLE 4. Values of measurements and percent differences between physical and mCT sections in the recent sauropsid teeth

Measurement	<i>Alligator mississippiensis</i>			<i>Crocodylus palustris</i>		
	mCT	Physical	% Diff.	mCT	Physical	% Diff.
1	0.15	0.14	7.14%	0.18	0.19	5.26%
2	0.05	0.05	0.00%	0.24	0.24	0.00%
3	0.11	0.12	8.33%	0.20	0.21	4.76%
4	0.07	0.06	16.67%	0.18	0.17	5.88%
5	0.15	0.16	6.25%	0.14	0.15	6.67%
6	0.11	0.11	0.00%	0.17	0.16	6.25%
7	0.09	0.09	0.00%	0.13	0.13	0.00%
8	0.04	0.04	0.00%	0.15	0.17	11.76%
9				0.17	0.16	6.25%
10				0.13	0.12	8.33%
Average (Absolute Value)			4.80%			5.52%

TABLE 5. Comparison between measurements recorded on-screen using software and those recorded on printed images using a digitizing tablet

Measurement	<i>Homo sapiens</i> RM ₃			<i>Papio ursinus</i> LM ²			<i>Cebus apella</i> LM ₂		
	On-Screen	Digitizer	% Diff.	On-Screen	Digitizer	% Diff.	On-Screen	Digitizer	% Diff.
LCT	1.68	1.62	3.70%	n/a	n/a	n/a	0.57	0.54	5.56%
BCT	1.74	1.68	3.57%	1.47	1.39	5.76%	0.56	0.58	3.45%
MOB	1.47	1.43	2.80%	1.79	1.73	3.47%	0.40	0.42	4.76%
BCD	9.38	9.41	0.32%	11.83	11.79	0.34%	4.64	4.65	0.22%
Average (Absolute Value)			2.60%			3.19%			3.50%

scan; in this case, mCT was incapable of clearly distinguishing enamel from dentine (Fig. 4).

The 2.0-Myr-old *Papio robinsoni* molar demonstrates that enamel and dentine can be differentiated by mCT in a fossil when the enamel is of moderate thickness (0.5–1.0 mm). The relative inability of mCT to differentiate between enamel and dentine in the *Moschops* tooth, and its total inability to do so in the *Diademodon* tooth, may reflect the comparatively greater degree of fossilization (i.e., remineralization) of the enamel (and especially dentine) in these Karoo specimens.

However, geochronological age does not account entirely for differences in the ability of mCT to visualize enamel. The *Diademodon* tooth is approximately 22 Myr younger than the *Moschops* incisor. Nevertheless, it is possible to visualize the enamel cap of the *Moschops* specimen, whereas it is totally invisible to mCT in *Diademodon*. It is possible that diagenetic alteration, which may be (to some degree) independent of geological age, may have differentially affected the *Moschops* and *Diademodon* teeth such that the remineralized dentine and enamel are of a more homogeneous structural composition in the former. In order to investigate this possibility, these two teeth were subjected to energy-dispersive X-ray microanalysis to investigate the composition of the dentine and enamel. The physical section faces of each specimen were examined in a LEO 1550 (LEO/Zeiss) SEM equipped with an EDAX Sapphire Si(Li) detector and Phoenix analyzer (EDAX) at 15 kV, zero tilt, a 4.1 takeoff, and a working distance of 8.0 mm. The results of these analyses are depicted in Figure 6. In the *Moschops* incisor, the dentine and enamel have essentially identical proportions of calcium and phosphorus (i.e., typical calcium phosphate), and they differ only in the amount of silicon present. In the *Diademodon* tooth,

while calcium and phosphorus predominate the mineral chemistry of the dentine, the enamel is wholly lacking in phosphorus (it also exhibits some manganese). Thus, the dentine and enamel are dissimilar to one another in chemical composition in both specimens, although diagenetic alteration has not been the same in each. The introduction of silicon into the dentine compartment of the *Moschops* incisor (presumably in the form of quartz) might be expected to affect the mCT X-ray beam attenuation as much as the diagenetic loss of phosphorus from the enamel compartment of the *Diademodon* crown, which suggests an increase in porosity.

This appears to suggest that neither geological age per se nor the differential diagenetic alteration of the chemical composition of the enamel and dentine adequately explains the differences in the ability of mCT to visualize the enamel caps of the two therapsid teeth. Rather, the difference between them in the detection of enamel via mCT seems to be related principally to its absolute thickness. Enamel in *Moschops* is approximately six times thicker than in *Diademodon* (~0.30 mm in *Moschops* vs. ~0.05 mm in *Diademodon*). However, the inability of mCT to resolve the enamel cap in *Moschops* as clearly as in recent and substantially younger fossil teeth may be related to the diagenetic alterations of the dentine in the former.

DISCUSSION

The percent differences (mean = 3.52%) reported here between enamel thickness measurements derived from mCT scans and physical sections of recent teeth are significantly improved over standard CT procedures (7–34%) (Grine, 1991) and especially over lateral dental radiographs (15–115%) (Grine et al., 2001). The percent differ-

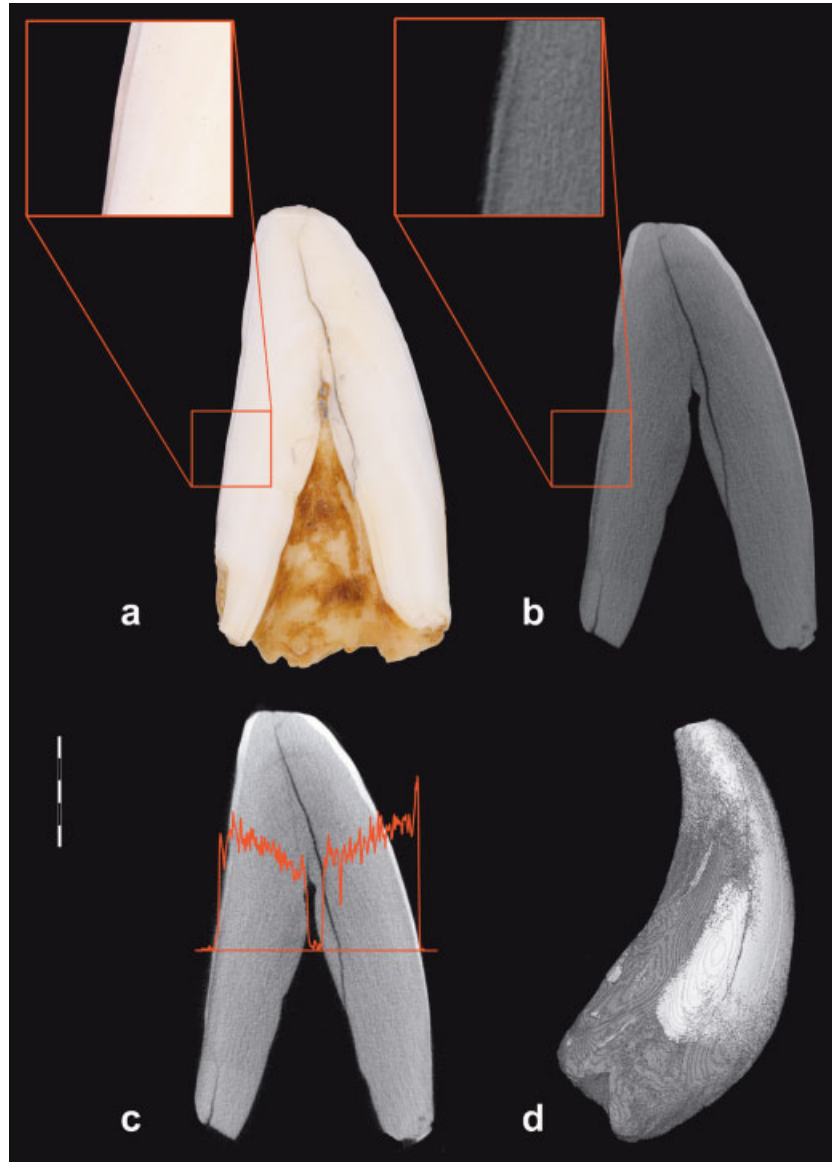


Fig. 5. Different visualizations of an *Alligator* tooth. Scale bar at left is 5 mm and applies to images a–c (image d is not to scale). **a:** Physical section with enlargement (box) showing the lingual enamel. **b:** mCT-derived section through the same plane with enlargement (box) showing that the lingual enamel can be differentiated from the underlying dentine by the human eye. **c:** An ROI line demonstrating that while the thicker enamel on the labial side of the tooth can be differentiated by segmen-

tation software as a peak in the intensity of the pixel values at the right side of the line, the thin enamel on the lingual surface of the tooth cannot be differentiated (note the absence of any intensity peak at left). **d:** A 3D computer volume rendering of the tooth, demonstrating that the enamel on the lingual surface is not distinguished from the underlying dentine by segmentation software.

ences obtained here are comparable to those recorded in studies comparing mCT scans and physical sections of trabecular bone (Müller et al., 1996a,b, 1998). This indicates that mCT is a valuable technique for the nondestructive assessment of enamel thickness in extant primate teeth. Figure 1 demonstrates the similarity between mCT and physical sections measured in this study, where only slight differences in the shapes of these sections are apparent.

The percent difference for the measurements reported here apparently does not relate to the thickness of the

enamel or the size of a given specimen (Tables 3 and 4). We suggest that the differences are due to human error in the process of measuring the photographs and printed images of the sections, rather than any inherent differences in the comparability of the two sections measured for each tooth or to any other factor having to do with specimen size or thickness.

Although distances measured on the computer screen by way of drawing lines did not differ substantially from those taken by hand using a digitizing tablet (Table 5), the mCT technology used here does appear to be limited in its

TABLE 6. Values of measurements and percent differences between physical and mCT sections in fossil teeth

Measurement	<i>Moschops capensis</i>			<i>Papio robinsoni</i>		
	mCT	Physical	% Diff.	mCT	Physical	% Diff.
1.00	0.32	0.33	3.03%			
2.00	0.33	0.34	2.94%			
3.00	0.26	0.27	3.70%			
4.00	0.27	0.28	3.57%			
5.00	0.32	0.33	3.03%			
6.00	0.33	0.36	8.33%			
7.00	0.32	0.33	3.03%			
BCD				10.13	10.01	1.20%
L1				0.63	0.61	3.28%
L2				0.59	0.63	6.35%
L3				0.63	0.60	5.00%
B1				0.42	0.40	5.00%
B2				0.82	0.84	2.38%
B3				0.92	0.91	1.10%
Average (Absolute Value)			3.95%			3.47%

ability to distinguish enamel from dentine when the enamel is very thin and/or when these two dental tissues have undergone diagenetic alteration. Thus, the extant sauropsid teeth and the *Ateles* and *Chiropotes* molars examined here demonstrate that mCT is capable of differentiating between enamel and dentine in recent specimens with thin enamel (as thin as 0.04 mm in the *Alligator* tooth). However, as is evident from the ROI line across the *Alligator* tooth (Fig. 5), whereas the pixel values clearly differentiate the thicker enamel, the extremely thin lingual enamel (ca. 0.04 mm) is not clearly distinguished from the adjacent dentine. Thus, it would appear that absolutely thin enamel (less than ~ 0.10 mm) is difficult to resolve adequately with mCT based on pixel values alone. Nevertheless, while it is not distinguished from dentine based on pixel values, the thin lingual enamel of the *Alligator* tooth is visible to the human eye in the mCT scans (e.g., Fig. 5). Since the comparably thin enamel of the *Diademodon* is not visible in terms of pixel values or to the human eye, this problem appears to be exacerbated by diagenetic processes involved in fossilization. It is possible that other mCT systems, such as industrial mCT (e.g., Bush et al., 2004) and synchrotron mCT (Tafforeau, 2004; Tafforeau et al., 2006), may be better suited to imaging thinly enameled fossils.

The poor visualization of enamel by mCT in the ca. 250-Myr-old therapsids compared to the ca. 2.0-Myr-old papionin, and the somewhat lower contrast in pixels along the ROI in this specimen compared to recent teeth, suggest that diagenetic alteration, which may differ substantially with geochronological age, may have an impact on visualization based on mCT scanning. On the other hand, the differences in detection by mCT of the enamel caps of the two therapsid specimens suggest that the absolute thickness of enamel (0.30 mm in *Moschops* vs. 0.05 mm in *Diademodon*) is a more problematic issue. Finally, the ability of segmentation software to distinguish enamel and dentine differs in some cases from the ability of the human eye to detect the same two tissues. The thin enamel of the *Alligator* tooth (e.g., Fig. 5) demonstrates that while the human eye may detect and measure thin enamel on mCT scans, computer-automated tissue segmentation (based on pixel shade values) may fail to do so.

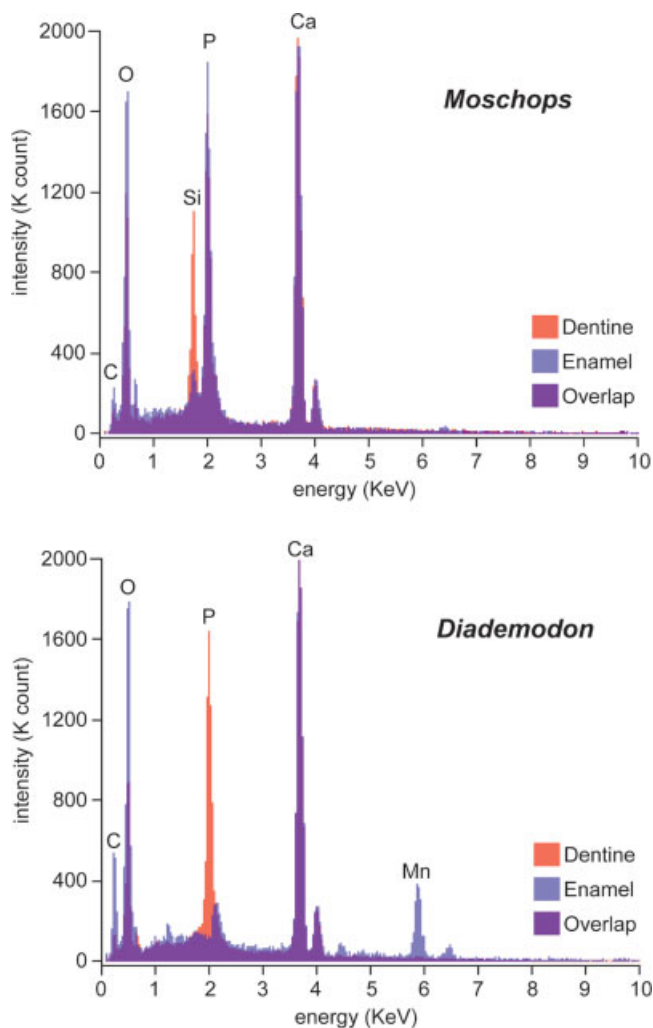


Fig. 6. Energy-dispersive X-ray microanalysis of enamel and dentine in the fossil therapsid teeth. Note that the composition of the enamel and dentine in *Moschops* are virtually identical except in the higher concentration of phosphorus in the former and the presence of silica in the latter. In *Diademodon*, the enamel and dentine differ in the presence of manganese in the former and the almost total absence of phosphorus in the latter.

Thus, the measurement of enamel thickness based on mCT scans by means of computer software alone may exacerbate the two problems of thin enamel and remineralization via diagenesis.

ACKNOWLEDGMENTS

The authors are grateful to R. Monk and J. Spence (Department of Mammalogy, American Museum of Natural History) for permission to mCT and section a molar of *Cebus apella*. Specimens were graciously loaned by R. Smith (South African Museum, Cape Town), J. Botha (National Museum, Bloemfontein), and P. Holroyd (University of California Museum of Paleontology, Berkeley). Information pertaining to these specimens was provided by E. Delson, B. Rubidge, and M. Raath. S. Judex and S. Xu provided access to and assistance with mCT facilities. J. Sipla, A. Kaufman, T. Smith, and S. Frank provided advice and assistance. We thank T. Radsbury for the discussion and we are grateful to L. Betti-Nash for the masterful execution of the illustrations. This manuscript benefited greatly from the comments and suggestions of J. Laitman and two anonymous reviewers.

LITERATURE CITED

- Alvesalo L, Tammisalo E. 1981. Enamel thickness in 45 X females permanent teeth. *Am J Hum Genet* 33:464–469.
- Alvesalo L. 1985. Dental growth in 47 XYY males and in conditions with other sex-chromosome anomalies. In: Sandberg AA, editor. *The Y chromosome*. New York: Alan R. Liss. p 277–300.
- Alvesalo L, Tammisalo E, Hakola P. 1985. Enamel thickness in 47 XYY males' permanent teeth. *Ann Hum Biol* 12:421–427.
- Alvesalo L, Tammisalo E, Therman E. 1987. 47 XYY females, sex chromosomes, and tooth crown structures. *Hum Genet* 7:345–348.
- Avishai G, Müller R, Gabet Y, Bab I, Zilberman U, Smith P. 2004. New approach to quantifying developmental variation in the dentition using serial microtomographic imaging. *Microsc Res Tech* 65:263–269.
- Balto K, Müller R, Carrington DC, Dobeck J, Stashenko P. 2000. Quantification of periapical bone destruction in mice by micro-computed tomography. *J Dent Res* 79:35–40.
- Baum G, Greenwood I, Smirnow R. 1963. Observation of internal structures of tooth by ultrasonography. *Science* 139:495–496.
- Beynon AD, Wood BA. 1986. Variations in enamel thickness and structure in East African hominids. *Am J Phys Anthropol* 70:177–193.
- Beynon AD, Dean MC, Reid DJ. 1991. On thick and thin enamel in hominoids. *Am J Phys Anthropol* 86:295–309.
- Bonse U, Busch F, Gunnewig O, Beckmann F, Pahl R, Delling G, Hahn M, Graeff W. 1994. 3D computed X-ray tomography of human cancellous bone at 8 μm spatial and 10^{-4} energy resolution. *Bone Miner* 25:25–38.
- Brunet M, Guy F, Pilbeam D, Mackaye HT, Likius A, Ahounta D, Beauvilain A, Blondel C, Bocherens H, Boisserie JR, De Bonis L, Coppens Y, Dejax J, Denys C, Düringer P, Eisenmann VR, Fanone G, Fronty P, Geraads D, Lehmann T, Lihoreau F, Louchart A, Mahamat A, Merceron G, Mouchelin G, Otero O, Campomanes PP, De Leon MP, Rage JC, Sapanet M, Schuster M, Sudre J, Tassy P, Valentin X, Vignaud P, Viriot L, Zazzo A, Zollikofer C. 2002. A new hominid from the Upper Miocene of Chad, Central Africa. *Nature* 418:145–151.
- Bush EC, Simons EL, Allman JM. 2004. High-resolution computed tomography study of the cranium of a fossil anthropoid primate, *Parapithecus grangeri*: new insights into the evolutionary history of primate sensory systems. *Anat Rec A* 281A:1083–1087.
- Chaimanee Y, Jolly D, Benammi M, Tafforeau P, Duzer D, Moussa I, Jaeger JJ. 2003. A Middle Miocene hominoid from Thailand and orangutan origins. *Nature* 422:61–65.
- Conroy GC. 1991. Enamel thickness in South African australopithecines: noninvasive evaluation by computed tomography. *Paleont Afr* 28: 53–59.
- Conroy GC, Vanier MW. 1991. Noninvasive evaluation of enamel thickness and volume in South African australopithecines by computed tomography. *Am J Phys Anthropol* 12(Suppl):60.
- Conroy GC, Lichtman JW, Martin LB. 1995. Some observations on enamel thickness and enamel prism packing in the Miocene hominoid *Otavipithecus namibiensis*. *Am J Phys Anthropol* 98:595–600.
- Cooper DML, Matyas JR, Katzenberg MA, Hallgrímsson B. 2004. Comparison of microcomputed tomographic and microradiographic measurements of cortical bone porosity. *Calcif Tiss Int* 74:437–447.
- Dauphin Y. 1987. Some results on the dental enamel structure in fossil and recent reptiles. *CR Acad Sci II* 305:1217–1219.
- De Kock MO, Beukes NJ, Hancox PJ, Kirshvink JL, Rubidge BS, Ward PD. 2003. Permian-Triassic megnetostratigraphy in the Karoo Basin of South Africa. *Geochem Cosmochim Acta* 67:A77–A78.
- Delson E. 1984. Cercopithecoid biochronology of the African Pliocene-Pleistocene: correlation among eastern and southern hominid-bearing localities. *Cour Forsch Inst Senckenberg* 69:199–218.
- Delson E. 1988. Chronology of South African australopithecine sites. In: Grine FE, editor. *Evolutionary history of the "robust" Australopithecines*. New York: Aldine de Gruyter. p 317–324.
- Dumont ER. 1995. Enamel thickness and dietary adaptation among extant primates and chiropterans. *J Mammal* 76:1127–1136.
- Durand EP, Rügsegger P. 1991. Cancellous bone structure: analysis of high-resolution CT images with run-length method. *J Comp Assist Tomogr* 15:133–139.
- Faerman M, Kharitonov VM, Batsevich V, Zilberman U, Smith P. 1994. A Neanderthal infant from the Barakai Cave, western Caucasus. *J Hum Evol* 27:405–415.
- Fajardo RJ, Müller R. 2001. Three-dimensional analysis of non-human primate trabecular architecture using micro-computed tomography. *Am J Phys Anthropol* 115:327–336.
- Fajardo RJ, Ryan TM, Kappelman J. 2002. Assessing the accuracy of high-resolution X-ray computed tomography of primate trabecular bone by comparison with histological sections. *Am J Phys Anthropol* 118:1–10.
- Gantt DG. 1983. The enamel of Neogene hominoids: structural and phyletic implications. In: Ciochon RL, Corruccini RS, editors. *New interpretations of ape and human ancestry*. New York: Plenum Press. p 249–298.
- Gantt DG, Kappelman J, Ketcham RA, Alder ME, Deahl TH. 2003. 3D approach to interpret enamel thickness and volume. *Am J Phys Anthropol* 36(Suppl):99.
- Grine FE, Vrba ES, Cruickshank ARI. 1979. Enamel prisms and diphyodonty: linked apomorphies of Mammalia. *S Afr J Sci* 75:114–120.
- Grine FE, Martin L. 1988. Enamel thickness and development in *Australopithecus* and *Paranthropus*. In: Grine FE, editor. *Evolutionary history of the "robust" Australopithecines*. New York: Aldine de Gruyter. p 3–42.
- Grine FE. 1991. Computed tomography and the measurement of enamel thickness in extant hominoids: implications for its paleontological application. *Palaeont Afr* 28:61–69.
- Grine FE, Stevens NJ, Jungers WL. 2001. An evaluation of dental radiograph accuracy in the measurement of enamel thickness. *Archs Oral Biol* 46:1117–1125.
- Grine FE. 2002. Scaling of tooth enamel thickness, and molar crown size reduction in modern humans. *S Afr J Sci* 98:503–509.
- Grine FE. 2004. Geographic variation in tooth enamel thickness does not support Neanderthal involvement in the ancestry of modern Europeans. *S Afr J Sci* 100:389–394.
- Grine FE. 2005. Enamel thickness of deciduous and permanent molars in modern *Homo sapiens*. *Am J Phys Anthropol* 126:14–31.
- Grine FE, Spencer MA, Demes AB, Smith HF, Strait DS, Constant DA. 2005. Molar enamel thickness in the Chacma baboon, *Papio ursinus*. *Am J Phys Anthropol* 128:812–822.
- Gron P. 1960. A geometrical evaluation of image size in dental radiography. *J Dent Res* 39:289–301.
- Haile-Selassie Y. 2001. Late Miocene hominids from the Middle Awash, Ethiopia. *Nature* 412:178–181.

- Haile-Selassie Y, Suwa G, White TD. 2004. Late Miocene teeth from Middle Awash, Ethiopia, and early hominid dental evolution. *Science* 303:1503–1505.
- Hancox PJ, Rubidge BS. 2001. Breakthroughs in the biodiversity, biogeography, biostratigraphy, and basin analysis of the Beaufort group. *J Afr Earth Sci* 33:563–577.
- Harris EF, Hicks JD. 1998. Enamel thickness in maxillary human incisors: a radiographic assessment. *Archs Oral Biol* 43:825–831.
- Harris EF, Hicks JD, Barcroft BD. 1999. Absence of sexual dimorphism in enamel thickness of human deciduous molars. In: Mayhall JT, Heikkinen T, editors. *Dental morphology*. Oulu, Finland: Oulu University Press. p 338–349.
- Hildebrand T, Laib A, Müller R, Dequeker J, Rügsegger P. 1999. Direct three-dimensional morphometric analysis of human cancellous bone: microstructural data from spine, femur, iliac crest, and calcaneus. *J Bone Miner Res* 14:1167–1174.
- Kappelman J. 1998. Advances in three-dimensional data acquisition and analysis. In: Rosenberger AL, Fleagle JG, McHenry HM, Strasser E, editors. *Primate locomotion*. New York: Plenum. p 205–222.
- Kay RF. 1981. The nut-crackers: a new theory of the adaptations of the Ramapithecinae. *Am J Phys Anthropol* 55:141–151.
- Khera SC, Carpenter CW, Vetter JD, Staley RN. 1990. Anatomy of cusps of posterior teeth and their fracture potential. *J Prosthet Dent* 64:139–147.
- Kinney JH, Ryaby JT, Haupt DL, Lane NE. 1998. Three-dimensional in vivo morphometry of trabecular bone in the OVX rat model of osteoporosis. *Technol Health Care* 6:339–350.
- Kono RT, Suwa G, Tanijiri T. 2002. A three-dimensional analysis of enamel distribution patterns in human permanent first molars. *Archs Oral Biol* 47:867–875.
- Kono R. 2004. Molar enamel thickness and distribution patterns in extant great apes and humans: new insights based on a 3-dimensional whole crown perspective. *Anthropol Sci* 112:121–146.
- Kono-Takeuchi R, Suwa G, Kanazawa E, Tanijiri T. 1997. A new method of evaluating enamel thickness based on a three-dimensional measuring system. *Anthropol Sci* 105:217–229.
- Kuhn JL, Goldstein SA, Feldkamp LA, Goulet RW, Jesion G. 1990. Evaluation of a microcomputed tomography system to study trabecular bone structure. *J Orthoped Res* 8:833–842.
- Lees S. 1968. Specific acoustic impedance of enamel and dentine. *Archs Oral Biol* 13:1491–1500.
- Lees S, Barber FE. 1968. Looking into teeth with ultrasound. *Science* 161:477.
- Lees S. 1971. Ultrasonics in hard dental tissues. *Int Dent J* 21:403–417.
- Lucas SG. 1995. Towards dicynodont biochronology. *Albertina* 16:33–40.
- Macho GA, Thackeray JF. 1992. Computed-tomography and enamel thickness of maxillary molars of Plio-Pleistocene hominids from Sterkfontein, Swartkrans, and Kromdraai (South-Africa): an exploratory study. *Am J Phys Anthropol* 89:133–143.
- Macho GA, Berner ME. 1993. Enamel thickness of human maxillary molars reconsidered. *Am J Phys Anthropol* 92:189–200.
- Macho GA, Spears IR. 1999. Effects of loading on the biochemical behavior of molars of Homo, Pan, and Pongo. *Am J Phys Anthropol* 109:211–227.
- MacLatchy L, Müller R. 2002. A comparison of the femoral head and neck trabecular architecture of Galago and Perodicticus using micro-computed tomography (μ CT). *J Hum Evol* 43:89–105.
- Maev RG, Maximovskye YM, Denisova LA, Maeva EY, Denisov AA, Chrkova TD, Domyshv DA. 2000. Acoustic microscopy: a new method for investigation of dental tissues. *Stomatology* 79:14–19.
- Maev RG, Denisova LA, Maeva EY, Denisov AA. 2002. New data on histology and physico-mechanical properties of human tooth tissue obtained with acoustic microscopy. *Ultrasound Med Biol* 28:131–136.
- Martin LB. 1985. Significance of enamel thickness in hominoid evolution. *Nature* 314:260–263.
- Martin LB, Olejniczak AJ, Maas MC. 2003. Enamel thickness and microstructure in pitheciin primates, with comments on dietary adaptations of the middle Miocene hominoid Kenyapithecus. *J Hum Evol* 45:351–367.
- McErlain DD, Chhem RK, Bohay RN, Holdsworth DW. 2004. Micro-computed tomography of a 500-year-old tooth: technical note. *J Assoc Canad Radiol* 55:242–245.
- Mezava S, Kawato T, Yoshida K, Nozaki H, Saito T, Tomura K, Onozawa M. 1999. Evaluation of human tooth structure with the ultrasonic imaging technique. *J Oral Sci* 41:191–197.
- Miller GS. 1918. The Piltdown jaw. *Am J Phys Anthropol* 1:25–52.
- Molnar S, Gantt DG. 1977. Functional implications of primate enamel thickness. *Am J Phys Anthropol* 46:447–454.
- Molnar S, Hildebolt C, Molnar IM, Radovic J, Gravier M. 1993. Hominid enamel thickness: I, the Krapina Neandertals. *Am J Phys Anthropol* 92:131–138.
- Müller R. 2002. The Zürich experience: one decade of three-dimensional high-resolution computed tomography. *Topics Magnet Resonance Imag* 13:307–322.
- Müller R. 2003. Bone microarchitecture assessment: current and future trends. *Osteoporos Int* 14:89–99.
- Müller R, Koller B, Hildebrand T, Laib A, Gionollini S, Rügsegger P. 1996a. Resolution dependency of microstructural properties of cancellous bone based on three-dimensional μ -tomography. *Technol Health Care* 4:113–119.
- Müller R, Hahn M, Vogel M, Delling G, Rügsegger P. 1996b. Morphometric analysis of noninvasively assessed bone biopsies: comparison of high-resolution computed tomography and histologic sections. *Bone* 18:215–220.
- Müller R, Rügsegger P. 1997. Micro-tomographic imaging for the nondestructive evaluation of trabecular bone architecture. In: Meunier A, editor. *Bone research in biomechanics*. Amsterdam: IOS Press. p 61–79.
- Müller R, van Campenhout H, Van Damme B, Van der Perre G, Dequeker J, Hildebrand T, Rügsegger P. 1998. Morphometric analysis of human bone biopsies: a quantitative structural comparison of histological sections and micro-computed tomography. *Bone* 23:59–66.
- Nagatoshi K. 1990. Molar enamel thickness in European Miocene and extant Hominoidea. *Int J Primatol* 11:283–295.
- Olejniczak AJ, Grine FE. 2005. High resolution measurement of Neandertal tooth enamel thickness by micro-focal computed tomography. *S Afr J Sci* 101:219–220.
- Peck SD, Rowe JM, Briggs GAD. 1989. Studies on sound and carious enamel with the quantitative acoustic microscope. *J Dent Res* 68:107–112.
- Peters OA, Laib A, Rügsegger P, Barbakow F. 2000. Three-dimensional analysis of root canal geometry by high-resolution computed tomography. *J Dent Res* 79:1405–1409.
- Rhodes JS, Pitt-Ford TR, Lynch JA, Liepins PJ, Curtis RV. 1999. Micro-computed tomography: a new tool for experimental endodontology. *Int Endodont J* 32:165–170.
- Rosset A, Spadola L, Ratib O. 2004. OsiriX: an open-source software for navigating in multidimensional DICOM images. *J Digital Imag* 17:205–216.
- Rubidge BS. 2006. Re-uniting lost continents: fossil reptiles from the ancient Karoo and their wanderlust. *S Afr J Geol* (in press).
- Rügsegger P, Koller B, Müller R. 1996. A microtomographic system for the non-destructive evaluation of bone architecture. *Calcif Tissue Int* 58:24–29.
- Sato I, Shimada K, Handal JC, Lance V, Gasser RF. 1988. Morphology of the American alligator (*Alligator mississippiensis*) tooth: I, the fine-structure and analysis of the enamel. *Am Zool* 28:A78.
- Schillingburg HT, Grace CS. 1973. Thickness of enamel and dentine. *J S Calif Dent Assoc* 41:33–52.
- Schwartz GT, Thackeray JF, Reid C, van Reenan JF. 1998. Enamel thickness and the topography of the enamel-dentine junction in South African Plio-Pleistocene hominids with special reference to the Carabelli trait. *J Hum Evol* 35:523–542.
- Schwartz GT. 2000a. Enamel thickness and the helicoidal wear plane in modern human mandibular molars. *Archs Oral Biol* 45:401–409.
- Schwartz GT. 2000b. Taxonomic and functional aspects of the patterning of enamel thickness distribution in extant large-bodied hominoids. *Am J Phys Anthropol* 111:221–244.

- Senut B, Pickford M, Gommery D, Mein P, Cheboi K, Coppens Y. 2001. First hominid from the Miocene (Lukeino Formation, Kenya). *CR Acad Sci Ser II A* 332:137–144.
- Shellis RP, Beynon AD, Reid DJ, Hiiemae KM. 1998. Variations in molar enamel thickness among primates. *J Hum Evol* 35:507–522.
- Simons EL, Pilbeam D. 1972. Hominoid paleoprimateology. In: Tuttle R, editor. *The functional and evolutionary biology of primates*. Chicago: Aldine. p 36–62.
- Smith P, Zilberman U. 1994. Thin enamel and other tooth components in Neanderthals and other hominids. *Am J Phys Anthropol* 95:85–87.
- Smith RMH, Keyser AW. 1995. Biostratigraphy of the Tapinocephalus assemblage zone. In: Rubidge BS, editor. *SACS biostratigraphic series no 1*. Pretoria: Council for Geoscience. p 8–17.
- Spears IR, Macho GA. 1998. Biomechanical behaviour of modern human molars: implications for interpreting the fossil record. *Am J Phys Anthropol* 106:467–482.
- Sperber GH. 1985. Comparative primate dental enamel thickness. In: Tobias PV, editor. *Hominid evolution: past, present, and future*. New York: Alan R. Liss. p 443–454.
- Sperber GH. 1986. Palaeodontology: radiographic revelations of the Australopithecinae. In: Singer R, Lundy JK, editors. *Variation, culture, and evolution in African populations*. Johannesburg, South Africa: Witwatersrand University Press. p 195–207.
- Spoor CF, Zonneveld FW, Macho GA. 1993. Linear measurements of cortical bone and dental enamel by computed-tomography: applications and problems. *Am J Phys Anthropol* 91:469–484.
- Strait DS, Grine FE, Moniz MA. 1997. A reappraisal of early hominid phylogeny. *J Hum Evol* 32:17–82.
- Strait DS, Grine FE. 2001. The systematics of *Australopithecus garhi*. *Ludus Vitalis* 9:109–135.
- Strait DS, Grine FE. 2004. Inferring hominoid and early hominid phylogeny using craniodental characters: the role of fossil taxa. *J Hum Evol* 47:399–452.
- Stroud JL, Buschang PH, Goaz PW. 1994. Sexual dimorphism in mesiodistal dentine and enamel thickness. *Dent-Max-Fac Radiol* 23:169–171.
- Stroud JL, English J, Buschang PH. 1998. Enamel thickness of the posterior dentition: its implications for nonextraction treatment. *Angle Orthod* 68:141–146.
- Tafforeau P. 2004. Aspects phylogénétiques et fonctionnels de la microstructure de l'émail dentaire et de la structure tridimensionnelle des molaires chez les primates fossils et actuels: apports de la microtomographie é rayonnement X synchrotron. PhD thesis. Montpellier: Université de Montpellier II.
- Tafforeau P, Boistel R, Boller E, Bravin A, Brunet M, Chaimanee Y, Cloetens P, Feist M, Hoeszowska J, Jaeger J-J, Kay RF, Lazzari V, Marivaux L, Nel A, Nemoz C, Thibault X, Vignaud P, Zabler S. 2006. Applications of X-Ray synchrotron microtomography for non-destructive studies of paleontological specimens. *Appl Phys A* (in press).
- von Stechow D, Balto K, Stashenko P, Müller R. 2003. Three-dimensional quantitation of periradicular bone destruction by micro-computed tomography. *J Endodont* 29:252–256.
- White TD, Suwa G, Asfaw B. 1994. *Australopithecus ramidus*, a new species of early hominid from Aramis, Ethiopia. *Nature* 371:306–312.
- Witmer LM, Chatterjee S, Franzosa J, Rowe T. 2003. Neuroanatomy of flying reptiles and implications for flight, posture, and behavior. *Nature* 425:950–953.
- Wolpoff MH, Senut B, Pickford M, Hawks J. 2002. Sahelanthropus or "Sahelpithecus"? *Nature* 419:581–582.
- Yang Z. 1991. Ultrasound surface imaging and the measurement of tooth enamel thickness. PhD dissertation. Manchester: University of Manchester.
- Yang Z. 1996. Tooth enamel surface imaging measurement by ultrasound imaging method. *J Acoust Soc Am* 100:2710.
- Zilberman U, Smith P, Sperber GH. 1990. Components of australopithecine teeth, a radiographic study. *J Hum Evol* 5:515–529.
- Zilberman U, Smith P. 1992a. A comparison of tooth structure in Neanderthals and early *Homo sapiens sapiens*: a radiographic study. *J Anat* 180:387–393.
- Zilberman U, Smith P. 1992b. Evolutionary trends in hominid tooth components: a radiographic study. In: Smith P, Tchernov E, editors. *Structure, function, and evolution of teeth*. London: Freund. p 349–359.
- Zilberman U, Skinner M, Smith P. 1992. Tooth components of mandibular deciduous molars of *Homo sapiens sapiens* and *Homo sapiens neanderthalensis*: a radiographic study. *Am J Phys Anthropol* 87:255–262.
- Zilberman U, Smith P. 1994. Sex discrimination using tooth components measured from bite-wing radiographs. *Am J Phys Anthropol* 94:214.
- Zonneveld FW, Wind J. 1985. High resolution computed tomography of fossil hominid skulls: a new method and some results. In: Tobias PV, editor. *Hominid evolution: past, present, and future*. New York: Alan R. Liss. p 427–436.